

SURFACE MODIFICATION OF AISI 440B STAINLESS STEEL AND ITS INFLUENCE ON SURGICAL DRILL BITS PERFORMANCE

The development of modern invasive surgery is highly dependent on the performance of surgical instruments, understood as long-term efficiency arising from high resistance to wear and corrosion. In order to maintain sufficient reliability, surgical cutting instruments are often made of martensitic stainless steels. Nevertheless, the use of ferrous alloys in medical applications is still a concern due to their questionable corrosion and wear resistance. To extend their biocompatibility, improve stability in variable environmental conditions, improve ease of handling, and maximize their performance, diffusion layers and coatings are applied to the surface. The aim of this work was to evaluate the effect of TiN and diamond-like carbon (DLC) surface modification on the performance of surgical drill bits, that is, wear and corrosion resistance, measured in model and field tests. Based on the findings presented, DLC layers can be recommended as anti-wear and anti-corrosion coatings for surgical drill bits.

Keywords: surgical drill bits, corrosion, wear, DLC, TiN

1. Introduction

Surgical procedures that affect the human body's bone structure, such as total hip replacement, usually require drilling. Intermittent contact with hard tissues and body fluids as well as the need to undergo numerous sterilization processes comprise hard service conditions. The development of modern invasive surgery is highly dependent on the performance of surgical instruments, understood as long-term efficiency arising from high resistance to wear and corrosion. Taking into consideration the complexity, manufacturing costs, and diversity of contemporary surgical instruments, providing reliable and durable medical devices is an issue of great significance [1-2].

Instruments designed to make contact with bone tissue, for example, saws, drills, and chisels, are among the medical devices that are most exposed to tribological wear. As early as after only a few operational procedures, their geometry changes, pre-sharpened edges become rounded, and sometimes it is even possible to observe material chipping [1, 3]. This may cause problems with their handling or even contribute to the generation of temperatures that are far too high during drilling, which results in bone necrosis [4-6].

In order to maintain sufficient reliability, surgical cutting instruments are often made of martensitic stainless steels [7]. Nevertheless, the use of ferrous alloys in medical applications is still a concern due to their questionable corrosion and wear resistance. To extend their biocompatibility, improve stability in variable environmental conditions, improve ease of handling, and maximize their performance, diffusion layers and coatings are applied to the surface [8, 9] Both diamond-like carbon (DLC) and titanium nitride (TiN) coatings are

considered to be promising surface modification techniques in biomedical applications [10-13].

DLC coatings are believed to be biocompatible with the human body [10, 14], chemically inert [10], and corrosion [11, 15] and wear [14, 16, 17] resistant. A number of studies describe the effect of DLC application in industry and above all in medicine positively [16, 18]. However, relatively little attention is paid to martensitic stainless steels – literature sources mainly consider the application of DLC carbon layers on austenitic stainless steels and titanium alloys.

According to Marciniak et al. [9] DLC layers magnetron-sputtered on X39Cr13 martensitic stainless steels provide excellent corrosion resistance of finished products. Marciniak et al. [2] have also investigated the effect of DLC deposition on the wear resistance of surgical drills. In the research, the cutting edges of surgical drills were compared before and after drilling a series of 1000 holes in the bovine femur. As the findings imply, successful application of DLC layers significantly improves resistance to wear of surgical cutting instruments, extending the service life of cutting devices. Moreover, it has been suggested that coatings obtained by the PACVD RF (Radio-Frequency Plasma-Assisted Chemical-Vapor Deposition) method present better mechanical properties than layers produced by magnetron sputtering.

As Biel-Golaska [19] states, DLC coatings stabilize the corrosion potential of X15Cr13 martensitic stainless steel in Ringer's solution. Microscopic observations of the steel in as-machined state and after application of the protective layer indicate that steel subjected to surface modification exhibits higher resistance to corrosion than raw material.

Nowadays, TiN layers are used as anti-wear, anti-corrosion, and decorative coatings and also as diffusion

* DEPARTMENT OF BIOMEDICAL ENGINEERING AND MATERIALS SCIENCE, BIALYSTOK UNIVERSITY OF TECHNOLOGY, FACULTY OF MECHANICAL ENGINEERING, WIEJSKA 45C STR., 15-644 BIALYSTOK, POLAND

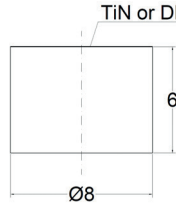
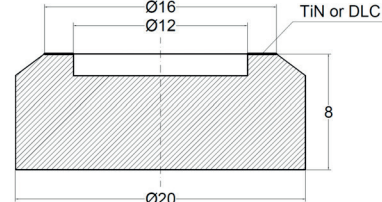
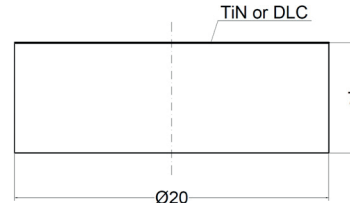
[#] Correspondence author: m.lepicka@pb.edu.pl

Chemical composition of AISI 440B martensitic stainless steel

	C	Mn	Si	S	P	Cr	Mo	V	Fe
EDX	n/o	0.74	0.84	–	0.03	19.25	0.98	0.09	balance
PN-EN 10088 -1:2005 [22]	0.85 ±0.95	max 1.00	max 1.00	max 0.040	max 0.030	17.00 ±19.00	0.90 ±1.30	0.07 ±0.12	balance

TABLE 2

Summary of analyzed samples; Q – quenching, T – tempering

Series no.	Heat treatment	Coating	Shape	Test type
1.1	Q + T in 250 °C	–		Corrosion test
1.2		DLC		
1.3		–		
1.4	Q + T in 500 °C	TiN		
2.1	Q + T in 250 °C	–		Tribological test – disc
2.2		DLC		
2.3	Q + T in 500 °C	TiN		
3.1	Q + T in 250 °C	–		Tribological test – plate
3.2		DLC		
3.3	Q + T in 500 °C	TiN		
4.1	Q + T in 250 °C	–	Fig. 2	Field test
4.2		DLC		
4.3		TiN		

barriers [20]. According to the literature, their main advantages are high hardness and wear resistance, chemical stability, and decorative properties [20]. For this reason, TiN coatings are encountered in a wide range of applications, such as protective layers on cutting tools, semi-conductor devices, and optical and biomedical products [12].

According to Biel-Golaska and Kalembe [8], in comparison to the untreated steel, the application of TiN layers on dental drills extends the service life of these tools up to six times. The advantageous influence of TiN layers on martensitic stainless steels has also been reported by Park et al. [21]. According to them, the application of TiN coating on X39Cr13 martensitic stainless steel results in significant improvement in the material's corrosion characteristics and hardness. They indicated that the cytotoxicity test was negative.

Taking into account the information provided, the aim of the study was to evaluate the effect of TiN and DLC surface modification on the performance of surgical drill bits, that is, the wear and corrosion resistance measured in model and field tests.

2. Materials

AISI 440B surgical stainless steel was selected as the substrate material. The chemical composition of the examined material is presented in TABLE 1.

The research material has been prepared according to the technological process applied for the manufacture of surgical drill bits. Specimens were heat treated and sandblasted and then selected coatings were applied (TABLE 2). TiN and DLC

layers were deposited by PVD (Physical Vapor Deposition) methods by HVM Plasma Ltd. (Czech Republic). The effect of the deposition of TiN and DLC layers on the corrosion and tribological properties of the selected steel was investigated. Moreover, the influence of the application of TiN and DLC layers on the performance of AISI 440B commercial surgical drill bits was analyzed.

3. Experimental methods

3.1. Materials characterization

The microstructures and surface morphologies of the samples were studied by scanning electron microscopy (SEM; S-3000N, Hitachi), optical microscopy (OM; BX51M, Olympus equipped with Olympus SC100 digital camera), and an energy-dispersive X-ray (EDX) analyzer (Thermo Noran).

Hardness measurements were performed using Vickers universal indenters (NEOPHOT 21, Carl Zeiss Jena). The thicknesses of DLC and TiN layers were evaluated using measurements made by confocal scanning microscope (CLSM; LEXT OLS 4000, Olympus). The as-received sample roughness was measured using a profilometer (Talysurf-10, Taylor-Hobson).

3.2. Corrosion tests

Corrosion tests were performed on a PGP201 potentiostat/galvanostat (Radiometer Analytical) equipped with VoltaMaster 4 software, which comprises an integral research kit. Potentiodynamic polarization scans and open-circuit potential (E_{OCp}) tests of metallic samples were carried out. A constant scan rate of 0.003 V/s was maintained during the potentiodynamic polarization scans. All corrosion tests were performed in 70 ml of an open-to-air physiological saline solution at room temperature (21 °C). The electrode set consisted of a saturated calomel electrode (SCE, 0.242 V at 25 °C versus SHE at 25 °C), platinum auxiliary electrode (31.4 mm² contact surface), and an AISI 440B martensitic stainless steel sample, whose circular area of 50.24 mm² was in contact with the testing solution. Using the software, the values of the corrosion potential (E_{corr}) and the corrosion current (i_{corr}) (Tafel method) were determined.

3.3. Tribological tests

Tribological tests were performed on a disc-on-plate tribometer (Fig. 1) working in an oscillating movement mode at a frequency of 1 Hz with a given initial gap between working surfaces. The research was conducted during the periodically variable motion with low velocity and variable values of pressure; 0.9% NaClaq solution was used as lubricant. Tribological tests lasted for 2 hours under the maximum load of 250 N. Friction coefficients were calculated from the maximum values of friction force to describe extreme resistances to motion. The geometry and dimensions of the tribological pair are shown in TABLE 2.

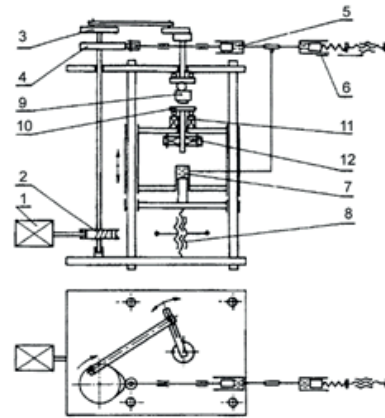


Fig. 1. Schematic diagram of the tribometer [23]: (1) electric motor; (2) gear; (3) crank mechanism; (4) cam; (5) hydraulic pump; (6) load governor; (7) hydraulic servo; (8) screw elevator; (9) specimen holder; (10) counter-specimen; (11) load transducer; (12) friction transducer

3.4. Field tests

In order to evaluate the effect of surface modification on the wear of surgical drill bits (Fig. 2), a study on cutting efforts when drilling porcine cortical bone was carried out. Tests were performed on a specially designed test stand consisting of a bench drill, which was equipped with a force sensor and force transducer, and a computer, on which friction torque changes during drilling were recorded. Femoral and shin bones were collected fresh from a local butchery and prepared a few days after 10-month-old piglets had been sacrificed. Forty holes were made with each bit. The total cutting depth of each bit was approximately 160×10^{-6} m. A constant load of 50 N and rotation speed $\omega = 350$ RPM were applied. Torque and drilling time were registered for each hole. No cutting fluids were used, just like during total hip replacement surgery. After drilling, the change in teeth geometry was measured on a Falcon QC (Quadra-Chek) three-axis non-contact video measuring machine.



Fig. 2. Surgical drill bits for field tests: (a) no surface modification, (b) DLC, (c) TiN

4. Results and discussion

4.1. Materials characterization

The microstructures of AISI 440B steel tempered at 250 and 500 °C are presented in Fig. 3. The cross-sections were taken in parallel to the rolling direction of the rod, from which the research material was cut. A typical distribution of primary carbides (Fig. 3a – PC) in the martensite solution of material

tempered at 250 °C is presented. A very fine, well-distributed network of ϵ -carbides, which precipitate during tempering, is noted. The high carbon (0.85–0.95%) and chromium (17–19%) contents induce carbide precipitation, so the steel becomes highly wear resistant. Due to deformation during the rolling process, the primary carbides are arranged in parallel lines, while transverse cracks are visible on some precipitates.

A similar picture is presented for steel tempered at 500 °C (Fig. 3b). Primary carbides (PC) and tempered sorbite precipitates are visible in the martensite solution. A fine network of corrosion characteristics of deteriorating secondary carbides is presented. As in Fig. 3a, transverse cracks of primary carbides are shown.

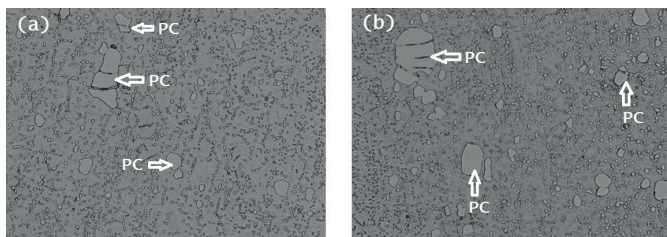


Fig. 3. AISI 440B surgical stainless steel microstructure: (a) tempered at 250 °C, (b) tempered at 500 °C. OM microphotographs, 200× magnification

TABLE 3 gives the fundamental characteristics of the obtained layers. According to the results, the DLC layer was significantly harder than the TiN coating. In research by Field et al. [24] it was stressed that DLC coatings are significantly harder and exhibit a lower coefficient of friction than nitride-based layers. The hardness of DLC layers is highly dependent on the generation methods and conditions, and their high hardness is usually explained by the high fraction of sp^3 bonds. In DLC coatings, the sp^3 bonds are responsible for the hardness, fracture toughness, tribological properties, and electrochemical and chemical inertness [17]. The thickness of the DLC layer and the surface roughness were about half of those of TiN.

TABLE 3

General characteristics of the obtained layers

Series no.	Layer type	Hardness HV0.1	Thickness [μm]	Roughness Ra [μm]
1.1	Reference (no coating)	740	–	0.25
1.2	DLC	2272	0.685	0.25
1.4	TiN	1465	1.085	0.60

4.2. Corrosion tests

The change in the E_{OCP} (free corrosion potential) of the analyzed specimens over time is presented in Fig. 4. As can be seen in Fig. 4, the initial potential of DLC-coated series is the most positive among all the examined samples. This implies that application of the DLC layer results in enhancement of the chemical stability of AISI 440B stainless steel in physiological fluids. According to the literature, the superb anticorrosive properties of DLC layers are attributed to their high density and low porosity. Due to their lower porosity, the passage of

corrosive solution into the coating is inhibited [25] and the oxygen diffusion is reduced [26]. Therefore, the tendency toward localized corrosion is depressed.

Furthermore, the curves of TiN and reference material (tempered at 500 °C) almost coincide, starting the potential drop from 300 ± 20 mV. The observed decrease in corrosion potential is related to the equilibrium processes, in which the corrosive dissolution is prevalent. In all cases, EOCV values stabilize after 80–100 minutes of immersion in physiological saline solution. During the free corrosion potential study, no corrosion pits were observed.

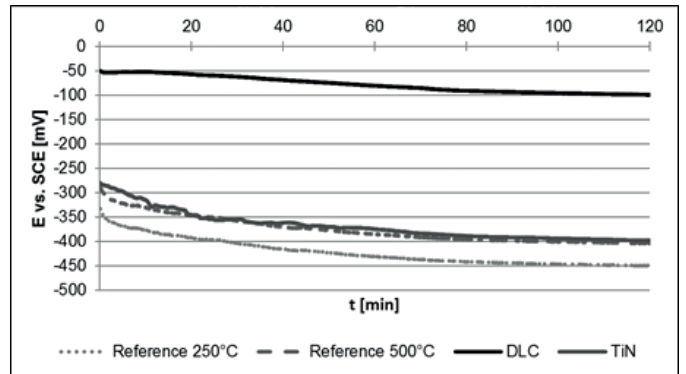


Fig. 4. Change of free corrosion potentials (E_{OCP}) over time

The corrosion behavior of AISI 440B samples during anodic polarization is given in Fig. 5. As depicted by the family of curves, significant differences in E_{corr} and i_{corr} values are achieved by each series. Above all, as in the open-circuit potential measurements, the curve that represents DLC surface modification differs remarkably from the other ones. In comparison with the reference material, a significant decrease in i_{corr} and a shift in corrosion potential towards positive values are observed. This implies that application of the DLC layer delays the onset of the corrosion processes on the finished product surface considerably.

In the case of the reference (500 °C) and TiN-modified series, overlapping of cathodic branches can be seen; minor differences in corrosion behavior between the series are noted in the anodic course. What is more, pitting potential can be noted. In the literature, the occurrence of pitting potential is attributed to the development of corrosion pits on the anodically polarized sample. Nevertheless, the polarization curves obtained for specimens are characteristic of uniform/general corrosion.

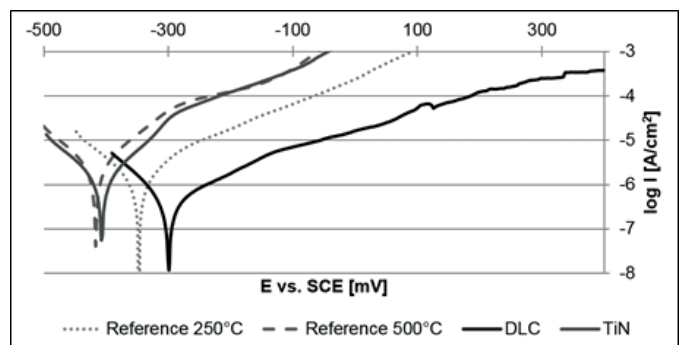


Fig. 5. Anodic polarization curves of analyzed samples

The post-test surface morphologies of TiN- and DLC-modified samples are presented in Fig. 6. Several corrosion pits were found on the TiN-modified AISI 440B steel (Fig. 6b), while the DLC-coated specimens (Fig. 6a) did not display signs of pitting corrosion.

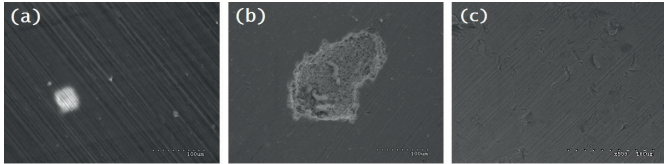


Fig. 6. AISI 440B surgical stainless steel microstructure: (a) DLC coated, (b) TiN coated, (c) reference, tempered at 500 °C. SEM microphotographs, 500× magnification

According to Liu et al. [25], the porosity and adhesion strength of coatings are two main factors affecting the corrosion resistance. Although chemically inert TiN layers are not involved in the corrosive dissolution processes, material coated with it can be severely pitted due to the occurrence of layer micro-imperfections on the detail's surface. According to the literature, TiN layers obtained by PVD methods are not free from structural defects in the form of pores, microcracks, and small holes [12, 20, 27]. The leakages into the layers and the pinholes through their thickness form contact channels between the aggressive medium and the surface, which significantly deteriorates the electrochemical properties of TiN coatings in aqueous media [12, 26]. According to Liu et al. [26], proper corrosion resistance of TiN-coated material is preserved until a system of cavities is formed under the layer. With the onset of corrosion cavities, the substrate can be undercut below the film and, at some point, areas adjacent to the micropores may collapse. In the research by Alkhateeb et al. [28], it was noted that TiN layers, even without external disturbance, were covered with microcracks. The occurrence of microcracks affected the corrosion performance of the investigated coatings, deteriorating the corrosion characteristics of the steel. Moreover, in a study by Li et al. [29], 1Cr11Ni2W2MoV martensitic steel coated with TiN exhibited superior corrosion resistance in long-term corrosion studies in NaCl and H₂SO₄ solutions until approximately the 100th hour of the experiment. After about 100 hours had elapsed, micropores appeared on the coating's surface, forming contact channels between the aggressive solutions and the steel.

4.3. Tribological tests

Wear studies indicated that DLC layers are characterized by a low value of friction coefficient (Fig. 7a) (average $\mu = 0.03$), which remained quite stable during the whole two-hour test. On the contrary, the friction coefficient of TiN-modified samples (Fig. 7b) rose until the end of the test, reaching up to ten times as high as that of DLC. Importantly, the analyzed layers were characterized by superb anti-wear properties. Unlike the reference material, DLC- and TiN-modified samples showed no measurable wear during the test. However, it should be noted that in the literature, cases of TiN fatigue cracking and spalling from martensitic stainless steels are described [11].

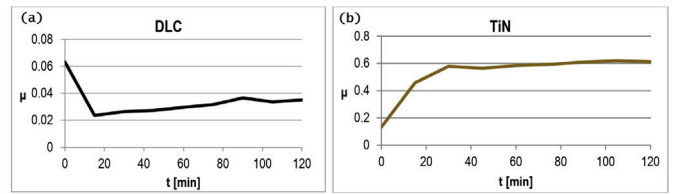


Fig. 7. Change in coefficient of friction over time: (a) DLC, (b) TiN

4.4. Field tests

As mentioned before, field tests were performed on a specially designed test stand (Fig. 8), consisting of a bench drill, which was equipped with a force sensor and force transducer, and a computer, on which changes in friction torque during drilling were recorded. A special holder for porcine bones was designed and manufactured to meet the needs of the study (Fig. 9).



Fig. 8. Test stand for field tests

In general, no direct correlation between the number of drilled holes and drilling time or axial torque was observed, as one would expect. Random variation of results was observed for all examined drills. This might be caused by the heterogeneity of bone tissue and external geometry of the cut material. The influence of anisotropy on the cutting of cortical bone has been discussed recently by some authors [30, 31]. It was shown that both chip morphology and temperature are affected by the anisotropy of the cortical bone during penetration processes [29]. Moreover, the uneven surface of the porcine bone could lead to the drill run-out observed during the experiment. The studies performed were of comparative nature and in this respect the results obtained can be considered reliable.

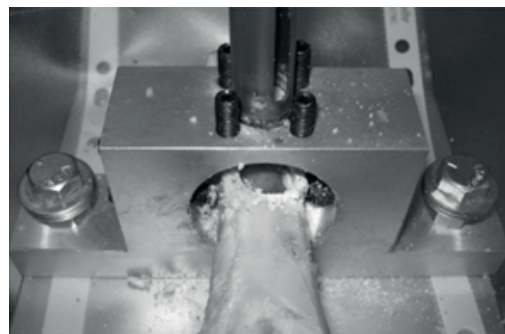


Fig. 9. Field tests of surface-modified surgical drill bits

According to the measurements of the change of teeth geometry (TABLE 4), the use of anti-wear layers led to

a remarkable improvement in the wear resistance of the surgical tools considered. Considering patient safety, wear reduction of surgical cutting and drilling instruments is a problem of high significance. When significant wear occurs and the sharpness of cutting lips is reduced, the cutting effort increases. High cutting effort during the drilling intervention causes microfractures in the bone adjacent to the cutting area [30]. What is more, during bone drilling, the bone temperature increases with multiple uses of the drill [6]. According to Soriano et al. [32] and Augustin et al. [5], one of the most damaging factors for bone regeneration is bone necrosis caused by excessive temperatures in the drilling site. In recent research by Karaca et al. [33], it was stated that TiBN-coated drills caused higher temperatures than uncoated ones, but no further discussion of the cause was provided. Ercoli et al. [34] investigated the performance of TiN-coated drills on bovine rib. According to the authors, TiN-coated drills showed greater wear and significantly lower material removal rates as compared to unmodified drills. A similar correlation between the overheating and layer modification was observed in this study. The temperature of drills coated with TiN rose significantly during cutting, accompanied by the characteristic smell of burnt bone.

TABLE 4
Changes in drill teeth geometry after drilling

Drill	Tooth height before drilling [mm]	Tooth height after drilling [mm]	Tooth wear [mm]
Unmodified	2.533	2.456	0.077
TiN	2.492	2.469	0.023
DLC	2.941	2.908	0.033

5. Conclusions

The aim of this work was to evaluate the effect of TiN and DLC surface modification on the performance of surgical drill bits, that is, the wear and corrosion resistance measured in model and field tests. The research material was prepared according to the technological process applied for the manufacture of surgical drill bits. Based on the findings presented, it can be stated that both TiN and DLC coatings significantly reduce the wear of AISI 440B surgical martensitic steel in field tests. However, based on the literature review and the obtained results, TiN layers do not provide superior corrosion resistance of the considered steel in model fluid. What is more, excessive heating of the TiN-modified drill was observed. Therefore, only DLC layers can be recommended as anti-wear and anti-corrosion coatings for surgical drill bits. However, further investigation of surface modification and its effect on bone temperature during drilling should be conducted.

Acknowledgement

This scientific work was supported by the Faculty of Mechanical Engineering, Bialystok University of Technology, project No MB/WM/10/2016.

REFERENCES

- [1] M. Gierzynska-Dolna, J. Adamus, J. Szyprowski, M. Sobocinski, *Eng. Biomater.* **33**, 102–106 (2003).
- [2] J. Marciniak, Z. Paszenda, M. Kaczmarek, J. Szewczenko, M. Basiaga, M. Gierzynska-Dolna, P. Lacki, *Maint. Probl.* **4**, 179–186 (2006).
- [3] Z. Paszenda, M. Basiaga, *Arch. Metall.* **36**, 103–109 (2009).
- [4] M. Basiaga, Z. Paszenda, J. Szewczenko, M. Kaczmarek, *Acta Bioeng. Biomech.* **13**, 29–36 (2011).
- [5] G. Augustin, T. Zigman, S. Davila, T. Udiljak, T. Staroveski, D. Brezak, S. Babic, *Clin. Biomech.* **27**, 313–325 (2012).
- [6] R.K. Pandey, S.S. Panda, *J. Clin. Orthop. Trauma* **4**, 15–30 (2013).
- [7] Z. Paszenda, J. Tyrlik-Held, *Instrumentarium chirurgiczne*. Wydawnictwo Politechniki Slaskiej, Gliwice (2003) [in Polish].
- [8] M. Biel-Golaska, I. Kalemba, *Prace Instytutu Odlewnictwa* **48**, 29–38 (2008).
- [9] J. Marciniak, Z. Paszenda, W. Walke, M. Basiaga, J. Smolik, *Arch. Mater. Sci. Eng.* **28**, 285–288 (2007).
- [10] M. Azzi, M.P. Amirault, M. Paquette, J.M. Klemberg-Sapieha, L. Martinu, *Surf. Coat. Technol.* **204**, 3986–3994 (2010).
- [11] L. Wang, J. Su, X. Nie, *Surf. Coat. Technol.* **205**, 1599–1605 (2010).
- [12] B. Subramanian, M. Jayachandran, *Mater. Lett.* **62**, 1727–1730 (2008).
- [13] T. Fraczek, M. Olejnik, *Surf. Eng.* **16**, 34–38 (2011).
- [14] R. Hauert, K. Thorwarth, G. Thorwarth, *Surf. Coat. Technol.* **233**, 119–130 (2013).
- [15] S.S. Hadinata, M.T. Lee, S.J. Pan, W.T. Tsai, C.Y. Tai, C.F. Shih, *Thin Solid Films* **259**, 412–416 (2013).
- [16] C.A. Love, R.B. Cook, T.J. Harvey, P.A. Dearnley, R.J. Wood, *Tribol. Int.* **63**, 141–150 (2013).
- [17] T. Morita, Y. Hirano, K. Asakura, T. Kumakiri, M. Ikenaga, C. Kagaya, *Mater. Sci. Eng. A – Struct.* **558**, 349–355 (2012).
- [18] G. Dearnaley, J.H. Arps, *Surf. Coat. Technol.* **200**, 2518–2524 (2005).
- [19] M. Biel-Golaska, *Prace instytutu odlewnictwa* **48**, 5–18 (2008).
- [20] C. He, J. Zhang, J. Wang, G. Ma, D. Zhao, Q. Cai, *Appl. Surf. Sci.* **276**, 667–671 (2013).
- [21] J. Park, D.J. Kim, Y.K. Kim, K.H. Lee, K.H. Lee, H. Lee, *Thin Solid Films* **435**, 102–107 (2003).
- [22] PN-EN 10088 -1:2005 Stainless steels. List of stainless steels.
- [23] M. Grądzka-Dahlke, J.R. Dąbrowski, B. Dąbrowski, *Wear* **263**, 1023–1029 (2007).
- [24] S.K. Field, M. Jarratt, D.G. Teer, *Tribol. Int.* **37**, 949–956 (2004).
- [25] H.G. Kim, S.H. Ahn, J.G. Kim, S.J. Park, K.R. Lee, *Diam. Relat. Mater.* **14**, 35–41 (2005).
- [26] C. Liu, G. Lin, D. Yang, M. Qi, *Surf. Coat. Technol.* **200**, 4011–4016 (2006).
- [27] A. Kagiya, K. Terakado, R. Urao, *Surf. Coat. Technol.* **169–170**, 397–400 (2003).
- [28] E. Alkhateeb, R. Ali, S. Virtanen, N. Popovska, *Surf. Coat. Technol.* **205**, 3006–3011 (2011).
- [29] Y. Li, L. Qu, F. Wang, *Corros. Sci.* **45**, 1367–1381 (2003).
- [30] C. Santiuste, M. Rodríguez-Millán, E. Giner, H. Miguélez, H. Compos. Struct. **116**, 423–431 (2014).

- [31] S. Li, A. Abdel-Wahab, E. Demirci, V.V. Silberschmidt, J. Biomech. **47**, 1117–1126 (2014).
- [32] J. Soriano, A. Garay, P. Aristimuño, P.J. Arrazola, Int. J. Adv. Manuf. Technol. **74**, 615–627 (2014).
- [33] F. Karaca, B. Aksakal, M. Kom, Med. Eng. Phys. **33**, 1221–1227 (2011).
- [34] C. Ercoli, P.D. Funkenbusch, H.J. Lee, M.E. Moss, G.N. Graser, Int. J. Oral Maxillofac. Implant. **19**, 335–349 (2004).

